RSC Advances

PAPER

View Article Online
View Journal | View Issue

Cite this: *RSC Adv.*, 2022, **12**, 3380

Acridine-based dyes as high-performance near-infrared Raman reporter molecules for cell imaging†

Jiasheng Du,‡ Jinming Li,‡ Yuzhan Li, Dong Wang, Hui Cao, Wanli He and Yang Zhou *

Received 4th December 2021
Accepted 14th January 2022

DOI: 10.1039/d1ra08827k

rsc.li/rsc-advances

A surface-enhanced Raman scattering (SERS) nanoprobe has been proven to be a promising tool for near-infrared (NIR) biomedical imaging and diagnosis because of its high sensitivity and selectivity. However, the development of NIR SERS reporters has been a bottleneck impeding the preparation of ultrasensitive SERS probes. Herein, we report the design and synthesis of a series of SERS reporters in the NIR region based on 10-methylacridine (AD). The AD nanotags (gold nanostar–AD molecules–BSA, AuNS–AD–BSA) exhibit appreciable SERS signals and can be detected at as low as the sub-picomole level. The results of *in vitro* imaging experiments show that it can be used in live-cell delineation.

Introduction

Surface-enhanced Raman spectroscopy (SERS) in biomedical applications has attracted growing attention because of its excellent sensitivity and selectivity. To generate highly sensitive Raman signals, it is crucial to choose Raman reporters with the desired optical properties.[1] Taking advantage of the chemical enhancement in surface-enhanced resonance Raman scattering (SERRS), the resonance effect between the electronic absorbance band of the Raman reporters and the excitation wavelength of the laser source can be improved, allowing for the increase of SERS signals by 10- to 100-fold.[2,3] Furthermore, in the biomedical field, NIR lasers are preferred for SERS-based detection because of their weak autofluorescence and photobleaching in the NIR window.[2,4–11]

However, there are only a few available Raman reporter molecules of which maximum absorption wavelength is resonant with NIR laser.[12–16] An effective strategy to redshift the absorption wavelength is to introduce proper chromophores to extend the conjugated structure. Unfortunately, most chromophores lead to high fluorescence background, which may cover the Raman signal. Mahmood *et al.*[17] and Yan *et al.*[18] developed a library of dyes with a *N*-substituted acridinium moiety exhibiting a moderate or even no emission of fluorescence. Yang *et al.*[19,20] reported that the introduction of a 10-methylacridine substituent accounts for a redshift of the maximum absorption wavelength. Although the acridine compounds induce a redshift in the visible region and enable an intense Raman signal, the dyes cannot produce SERS effect in the NIR region.

In this work, we designed and synthesized a series of polymethine dyes with donor–acceptor–donor (D–A–D) structures based on 10-methylacridine substituents. The dyes (CnAD dyes) were prepared in high yield, which exhibited good stability and maximum absorption wavelengths in the NIR region. Gold nanostar (AuNS) were used to modify the dyes, allowing for an extra enhancement *via* SERRS and resulting in a strong signal and high sensitivity to a 785 nm excitation. The limits of detection (LOD) of the nanotags can be detected in the sub-picomole range. The SERS images indicate the potential of AuNS–C5AD–BSA (gold nanostar–C5AD dye–BSA) in live cancer cell SERS imaging.

Experimental

Materials

Dichloromethane (DCM), methanol (MeOH), ethyl acetate (EtOAc) and acetic acid were purchased from Peking Reagent. Hydrogen tetrachloroaurate hydrate ($HAuCl_4 \cdot 4H_2O$), ammonia water, and acetic anhydride (Ac_2O) were obtained from Sinopharm Chemical Reagent Co., Ltd. Trisodium citrate dihydrate was obtained from Beijing Chemical Works. Zinc chloride ($ZnCl_2$, 98%), acetonitrile (99%) and *N*,*N*-diphenylformamidine (98%) were obtained from Macklin. Silver nitrate ($AgNO_3$, 99%) was obtained from GHTECH. Diphenylamine (99%), magnesium sulfate (99.5%), sodium acetate (AcONa, 99%), methyl iodide, *N*-[5-(phenylamino)-2,4-pentadienylidene]aniline monohydrochloride (98%) and PEG-SH (average molecular weight, 5000 g mol^{-1}) were obtained from J&K science. Ascorbic acid (AA, >99.0%), 3,3′-diethylthiatricarbocyanine iodide (DTTC) and

Department of Materials Physics and Chemistry, School of Materials Science and Engineering, University of Science and Technology Beijing, Beijing 100083, China

† Electronic supplementary information (ESI) available. See DOI: 10.1039/d1ra08827k

‡ Equal contribution.

bovine serum albumin (BSA) were obtained from Aladdin. Calcein-AM/PI cell cytotoxicity assay kit were obtained from Beyotime Institute of Biotechnology (China). DMEM, OPTI-MEM and phosphate buffered saline (PBS) were purchased from GIBCO Invitrogen Corp.

Instruments

Transmission electron microscopy (TEM, JEM-1200EX, JEOL, Japan) was used to characterize morphologies of the AD nanotags. Dynamic light scattering (DLS) and zeta potential were measured using Zetasizer Nano-ZS (Malvern, UK). Absorption properties of the nanoparticles was measured using a UV-vis-NIR spectrophotometer (V-570, Jasco, Japan). SERS measurements were recorded on a confocal Raman microscope (inVia Reflex, Renishaw, UK) equipped with a 785 nm laser. The Raman measurements of AD and DTTC nanotags were conducted using the following parameters: 50 L × objective lens, 0.85 mW laser power, and 10 s exposure time. The limit of detection (LOD) was evaluated *via* 50 L × objective lens with 1.7 mW laser power and 10 s exposure time. The SERS images of AD nanotags were acquired under a 5× objective lens with 1.7 mW laser power on the samples, 2 s exposure time and 50 μm step size. The *in vitro* cell SERS imaging was carried out using a 100× objective lens at 8.5 mW laser power with 5 s exposure time and 3 μm step size. The SERS images of nanotags and cells were created with the intensity of 1277 cm^{-1} SERS band after removing the baseline *via* wire 5.1.

Reporter library synthesis and properties

Synthesis of 9-methylacridine. *N*,*N*-Diphenylamine (5.0 g, 30 mmol), acetic acid (5.0 g, 84 mmol) and zinc chloride (21.3 g, 156 mmol) were stirred at 150 °C until the solids were completely dissolved. Then, the mixture was heated at 215 °C for 5 h. After cooling to ambient temperature, the mixture was heated again until melted and then was poured into ice water. The product was alkalized using ammonia water and was extracted using EtOAc. The organic layer was dried with $MgSO_4$ and purified by silica gel chromatography (DCM/EtOAc = 5 : 1) to give pure 1 (4.2 g, mmol, 72% yield). δ_H (500 MHz, $CDCl_3$) 8.29 (2H, d), 8.26 (2H, d, *J* 8.7), 7.80 (2H, t, *J* 8.1, 6.6, 1.4), 7.59 (2H, t), 3.16 (3H, s). EI-MS: *m*/*z* 194.09.

Synthesis of 9,10-dimethylacridin-10-ium iodide. Selenophene-2-carbaldehyde (1.0 g, 5 mmol) and methyl iodide (1.4 g, 10 mmol) were dissolved in acetonitrile (10 mL) and the reaction was refluxed for 12 h. The mixture was cooled to ambient temperature and filtered. Then, the product was isolated by crystallization from acetonitrile and methanol to afford 2(0.98 g, 2.9 mmol, 59% yield). δ_H (500 MHz, DMSO) 8.93 (2H, d, *J* 8.9), 8.77 (2H, d, *J* 9.2), 8.44 (2H, t, *J* 8.1), 8.03 (2H, t, *J* 7.9), 4.83 (3H, s), 3.53 (3H, s). ESI-MS: *m*/*z* 208.11 $[M]^+$.

Synthesis of (*E*)-10-methyl-9-(3-(10-methylacridin-9(10*H*)-ylidene)prop-1-en-1-yl)acridin-10-ium (C3AD). 9,10-Dimethylacridin-10-ium iodide (ADI, 2) (50.0 mg, 0.150 mmol, 1.0 equiv.), (*E*)-*N*,*N*-diphenylformamidine (14.7 mg, 0.075 mmol, 1.0 equiv.) and anhydrous sodium acetate (13.0 mg, 0.159 mmol, 2.0 equiv.) were dissolved in 20 mL acetic anhydride and heated to 80 °C for 2 hours under an argon atmosphere, then treated with 60 mL ether. Dye was purified by silica gel chromatography (DCM/MeOH = 10 : 1) to give pure C3AD (16.1 mg, 0.0379 mmol, 50.5% yield). δ_H (600 MHz, DMSO) 8.39 (4H, d, *J* 7.7), 8.07 (1H, d, *J* 9.0), 8.00 (4H, d, *J* 8.8), 7.93 (4H, d, *J* 7.9), 7.85 (1H, s), 7.58 (4H, t, *J* 7.6), 7.26 (1H, q, *J* 7.9, 7.1), 4.13 (6H, s). EI-MS: *m*/*z* 425.20 $[M]^+$.

Synthesis of 10-methyl-9-((1*E*,3*E*)-5-(10-methylacridin-9(10*H*)-ylidene)penta-1,3-dien-1-yl)acridin-10-ium (C5AD). 9,10-Dimethylacridin-10-ium iodide (ADI, 2) (50.0 mg, 0.150 mmol, 1.0 equiv.), malonaldehyde bis(phenylimine) (19.0 mg, 0.075 mmol, 1.0 equiv.) and anhydrous sodium acetate (13.0 mg, 0.159 mmol, 2.0 equiv.) were dissolved in 20 mL acetic anhydride and heated to 80 °C for 1.5 hours under argon atmosphere, then treated with 60 mL ether. Dye was purified by silica gel chromatography (DCM/MeOH = 10 : 1) to give pure C5AD (19.3 mg, 0.0428 mmol, 57.1% yield). δ_H (500 MHz, DMSO) 8.26 (4H, d, *J* 8.2), 8.05 (1H, t, *J* 9.0), 7.96 (4H, d, *J* 8.6), 7.89 (4H, m), 7.58 (1H, t, *J* 3.7), 7.53 (4H, d, *J* 7.7), 7.45 (2H, d, *J* 13.6), 7.10 (1H, t, *J* 12.3), 4.12 (6H, s). EI-MS: *m*/*z* 449.4 $[M]^+$.

Synthesis of 10-methyl-9-((1*E*,3*E*,5*E*)-7-(10-methylacridin-9(10*H*)-ylidene)hepta-1,3,5-trien-1-yl)acridin-10-ium (C7AD). 9,10-Dimethylacridin-10-ium iodide (ADI, 2) (50.0 mg, 0.150 mmol, 1.0 equiv.), *N*-[5-(phenylamino)-2,4-pentadienylidene]aniline monohydrochloride (21.3 mg, 0.075 mmol, 1.0 equiv.) and anhydrous sodium acetate (13.0 mg, 0.159 mmol, 2.0 equiv.) were dissolved in 20 mL acetic anhydride and heated to 80 °C for 1 hour under an argon atmosphere, then treated with 60 mL ether. Dye was purified by silica gel chromatography (DCM/MeOH = 10 : 1) to give pure C7AD (14.8 mg, 0.0310 mmol, 41.4% yield). δ_H (500 MHz, DMSO) 8.22 (4H, m), 7.97 (4H, m), 7.89 (4H, dd, *J* 7.9, 6.2), 7.53 (4H, m), 7.43 (2H, d, *J* 13.6), 7.29 (2H, d, *J* 12.6), 7.19 (1H, dd, *J* 26.4, 13.3), 6.85 (2H, t, *J* 12.7), 4.12 (6H, s). EI-MS: *m*/*z* 477.4 $[M]^+$.

Preparation of nanotags

Synthesis of gold nanostars. AuNSs were synthesized by seed-mediated growth.[21] The seed solution was prepared by adding 5 mL of 1 wt% citrate solution to 95 mL of boiling 0.5 mM $HAuCl_4$ solution under vigorous stirring. After 15 min of boiling, the solution was cooled down and stored at 4 °C. Then, 5 mL of the seed solution was added to 100 mL of $HAuCl_4$ solution (with 1.2 mL of 1 wt% $HAuCl_4$ and 100 μL of 1 M HCl), and then 1 mL of 3 mM $AgNO_3$ and 1 mL of 100 mM ascorbic acid were added. To stabilize the nanoparticle, we added 5 mL of 1 wt% citrate solution after the solution rapidly turns from light red to greenish. The concentration of nanoparticles was determined by UV-vis spectroscopy from the absorbance at 400 nm.[8,22]

Preparation and characterization of AuNS–AD–BSA. PEG-SH (0.1 mM) was added to avoid nanoparticle aggregation. To synthesize the AuNS–AD nanoparticles, the ethanol solution of dyes with different concentrations (2×10^{-4} to 2×10^{-9} M) were added into the AuNS ($[Au^0] \sim 0.6$ mM). After 3 h, the excess of dyes was removed by centrifugation at 3000 rpm for 15 min. Then, AuNS–AD–BSA were synthesized by mixing 100 μL 20 mg

mL^{-1} BSA for 1 h and washed by centrifugation at 3000 rpm for 15 min. AuNS–DTTC–BSA (with 2×10^{-5} M dyes, 500 μL) were synthesized as mentioned above.

Cell culture and biocompatibilities studies

A549 cells were cultured in DMEM medium containing 10% FBS and 1% penicillin/streptomycin at 37 °C in 5% CO_2. Cell survival rates of AuNS–C5AD-BSA were evaluated by MTT assays. 1×10^5 cells were seeded into 96-well plates and then allowed to grow for 24 h. The medium was replaced by fresh cell culture medium containing different concentrations (0, 20, 40, 80 and 100 μg mL^{-1}) of AuNS–C5AD-BSA. After incubation for 24 h, the medium was removed and the cells were washed with PBS. Subsequently, MTT was added into 96-well plates. After 4 h, the MTT was removed, 100 μL DMSO was added. Then, the absorbance was measured using a microplate reader.

Cellular SERS mapping

1×10^4 A549 cells were seeded onto quartz slides sitting on a 24-well plate overnight. After another 10 h-incubation of 1 mL culture medium containing AuNS–C5AD-BSA ([NP] ~ 1×10^9 NP mL^{-1}), cells were washed with PBS three times to remove medium and dissociative particles.

Results and discussion

Synthesis and characterization of dyes

The synthetic routes of AD dyes are shown in Fig. 1a, 9,10-dimethylacridin-10-ium iodide (**2**, ADI) was synthesized by iodomethane and 9-methylacridine (**1**, AD), which was prepared using diphenylamine and acetic acid. Acridine dyes were synthesized *via* a reaction between ADI and electrophile with good yield, ranging from 41.4% to 51.7%. The maximal absorbing wavelengths of C3AD and C5AD in CH_2Cl_2 are 804 nm and 908 nm, respectively. When the number of methine groups was increased, a redshift of approximately 100 nm of the absorption wavelengths was observed. In chloroform ($CHCl_3$) and ethanol (EtOH), the absorption peak around 804 nm was observed. In addition, there are two characteristic absorption peaks of C7AD in 804 nm and 1006 nm. AD dyes are better coplanar and tend to aggregate face-to-face in the solution (H-aggregation) with the increasing length of the polymethine chain. This phenomenon, with two close-maxima absorption peaks, arises from H-aggregation which leads to weaker fluorescence and facilitates Raman measurement.[17,23]

Synthesis and characterization of nanotags

AuNSs with a localized surface plasmon resonance (LSPR) band at around 730 nm were synthesized by seed-mediated growth.[21] Subsequently, ethanol solution containing different Raman reporters (C3AD, C5AD, and C7AD) at a concentration between 2×10^{-9} and 2×10^{-4} M were added to AuNSs, respectively. The reporter molecules were adsorbed to the negatively charged AuNSs surface through electrostatic interaction *via* the nitrogen atom.[24] Then, AuNS–AD (with 2×10^{-5} M dyes) was modified by BSA to improve biocompatibility. After modified with dyes and BSA, plasmon resonance absorption of nanotags was observed to redshift by ≈ 22 nm and ≈ 32 nm (Fig. S2a, d and f†). As shown in Fig. S2b, e and h,† after functionalization and modification, the hydrodynamic diameter increased ~26 nm and ~43 nm in the dominant peak compared with the pristine AuNSs. The zeta potential measurements showed that the

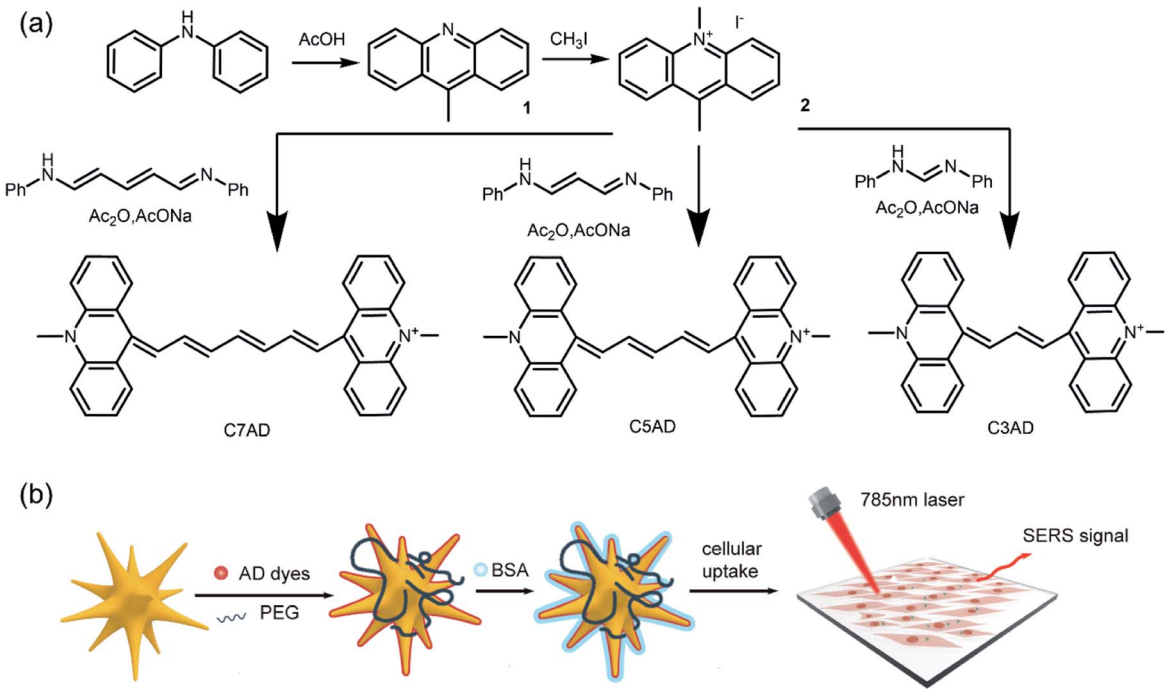

Fig. 1 (a) Synthetic routes of AD dyes. (b) Fabrication of NIR Raman reporter molecules modified SERS nanotags.

AuNS–AD was less negatively charged than that of the AuNSs, and that the addition of BSA also resulted in a decrease in negatively charged ions on the surface of AuNSs (Fig. S2c, f and i†). These results indicated that AuNSs were successfully coated with dyes and BSA. Transmission electron microscopy (TEM) was used to reveal the star-like structure of nanotags (Fig. S3†), which exhibited good monodispersity (Table 1).

SERS spectra and SERS nanotags with dyes

The nitrogen atoms in the acridine group provide a binding site for AuNSs. Since these AD dyes have similar structures, the fingerprint information of their Raman spectra highly overlaps. Weak signals of C=N stretching and C=C stretching appeared around 1600 cm^{-1}. Signals in the range of 1385–1415 cm^{-1} was attributed to the acridine stretching. Peaks around 1250–1277 cm^{-1} arise from the ring deformation of acridinium. Signals for C–H stretching vibrations at 700–900 cm^{-1} are visible. The signal around 400 cm^{-1} may refer to the bending of N–C=C.[25] These AD dyes, with similar SERS spectra, vary in the intensity of SERS nanotags. This confirms that Raman reporters lead to an extra signal enhancement when the absorption peak is resonant with laser source.

Table 1 The absorption maximum (λ_{max}) and yield of AD dyes

Dyes	Dye λ_{max} (CH_2Cl_2)	ε, 10^4 M^{-1} cm^{-1} (CH_2Cl_2)	Synthesis yield (%)
C3AD	804 nm	2.4	50.5
C5AD	908 nm (804 nm)	2.8	51.7
C7AD	804 nm (1006 nm)	8.2	41.4

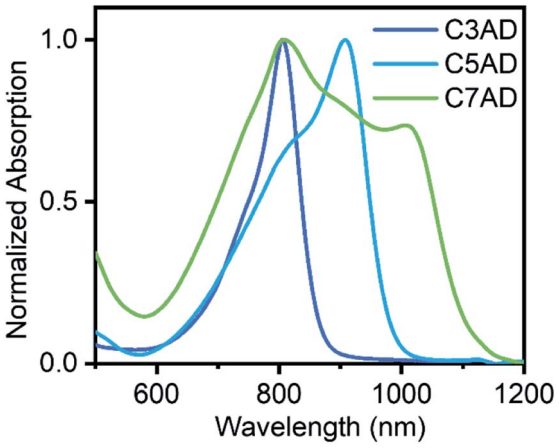

Fig. 3 UV-vis absorption spectra of C3AD, C5AD, and C7AD in CH_2Cl_2.

To fully estimate the SERS capabilities of AuNS–AD–BSA nanotags, the LODs was measured and AuNS–AD–BSA nanotags were compared with AuNS–DTTC–BSA nanotags. To study the LOD of the nanotags, AuNSs modified by proper concentration of dye molecules and BSA was synthesized and was diluted until no signal of the nanotags was observed. The peak at 1277 cm^{-1},

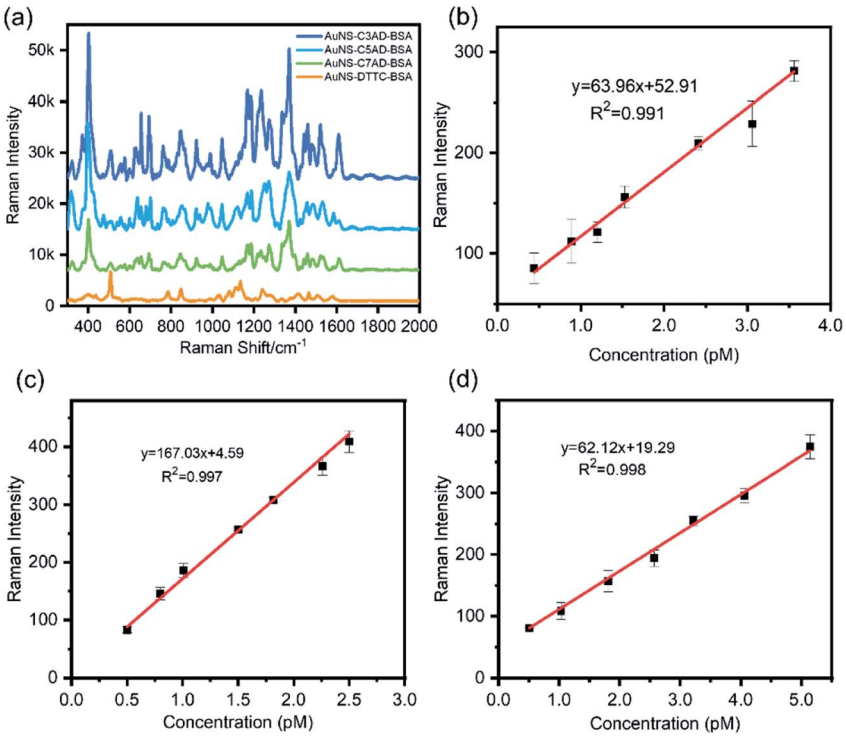

Fig. 2 (a) Comparison of SERS spectra between the commercial dye (DTTC) nanotag and the AD nanotags. The concentration of nanotags is 54 pM ($n = 3$). SERS intensities of the highest Raman peaks (400 cm^{-1} for AD dyes and 503 cm^{-1} for DTTC) are chosen to compute the contrast ratio. (b)–(d) SERS particle dilution studies for C3AD, C5AD and C7AD nanotags over the concentration range 0.4 pM to 5.4 pM. SERS intensity was determined by averaging the integrated intensity of the peak at 1277 cm^{-1} ($n = 3$).

which was one of the intense peaks in the spectrum, was used to calculate the LOD. LODs of nanotags were calculated to be approximately 0.4 pM, 0.50 pM, and 0.51 pM, respectively (n = 3). It shows a linear relationship between the concentration of nanotags and Raman intensity with good R^2 values (Fig. 2b–d, R^2 = 0.991, 0.997, and 0.998), indicating the possibility of quantitative analysis (Fig. 3).

After confirming the SERS sensitivity of the AuNS–AD–BSA nanotags, a commercial Raman reporter DTTC was chosen to substitute the synthesized dyes as the SERS reporter molecule. As shown in Fig. 2a, the contrast ratio between AuNS–AD–BSA nanotags and AuNS–DTTC–BSA nanotags expression was quantified to be approximately 1.7-fold to 4.7-fold based on the same test conditions. This difference may arise from the acridine group of Raman reporters and greater electromagnetic fields due to electrostatic interaction between organic salt and metal surface.[26]

In vitro experiments

***In vitro* SERS imaging of AD nanotags.** To evaluate *in vitro* SERS imaging performance of the nanotags, we conducted the SERS measurement on a glass capillary tube with a diameter of 0.1 mm. As shown in Fig. 4a, the SERS image became brighter as the concentration of nanotags increased from 0 to 259.1 pM. The results indicated that the AD nanotags have excellent SERS imaging capability when excited at 785 nm. As shown in Fig. 4b

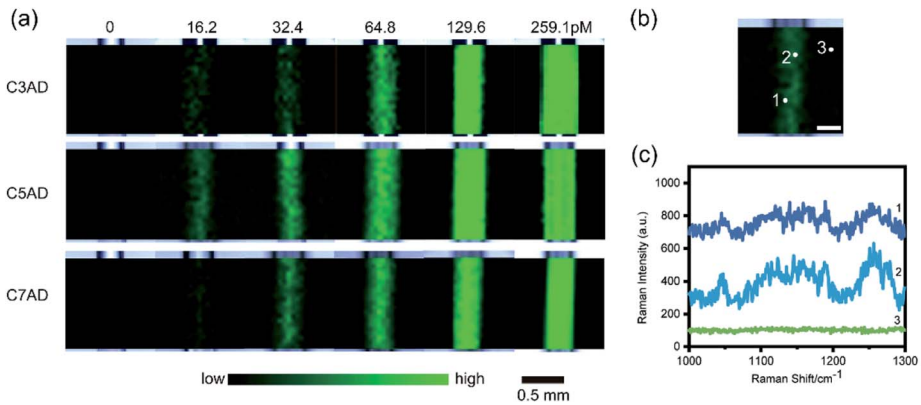

Fig. 4 (a) SERS images of AuNS–AD–BSA. (b) and (c) SERS images AuNS–C5AD–BSA and the corresponding SERS spectra of 16.2 pM inside the vessel (positions 1 and 2) and outside the vessel (position 3). Scale bar (white): 0.25 mm.

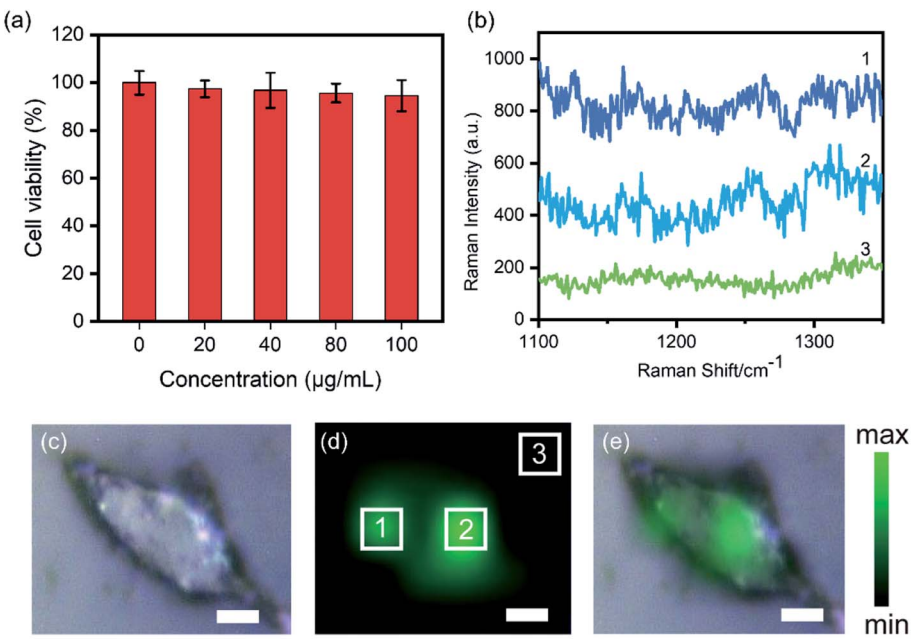

Fig. 5 (a) Cell viability of A549 after incubation with different concentrations of AuNS–C5AD–BSA for 12 h. (b) SERS spectra of position 1, 2, and 3 in (d) SERS mapping image. (c) Bright field image, (d) SERS mapping image, and (e) overlay of bright field image of A549 cell incubated with 1×10^9 NP mL^{-1} for 10 h. Scale bar: 5 μm.

and c, it is difficult to distinguish the peaks around 1250 cm^{-1} and 1277 cm^{-1}, referring to the acridine breathing, with the concentration of nanotags decreasing, which might be related to the noise of background and changes of anion in the solution.[26] The *in vivo* experiment of the AD nanotags reveals that the AuNS–C5AD–BSA exhibit stronger SERS signal under high fluorescent background of the glass. Therefore, the AuNS–C5AD–BSA was selected for cell imaging study.

***In vitro* SERS imaging of A549 cells.** We evaluated the safety and biocompatibility of the AuNS–C5AD–BSA *via* MTT assay. After A549 cells were incubated with various concentrations (0, 20, 40, 80, 100 μg mL^{-1}) of AuNS–C5AD–BSA for 12 h, no apparent toxicity was observed (Fig. 5a). We further assessed the *in vitro* SERS imaging capability of A549 cells using the AuNS–C5AD–BSA nanotags. As shown in Fig. 5d the SERS signal of C5AD was observed only inside the cell, while nearly no SERS signal was observed outside the cell. The signals are strong enough to delineate the live cells indicating that C5AD can be used as Raman reporter in SERS imaging of live cells.

Conclusions

In conclusion, we have designed and synthesized a set of NIR Raman reporters based on 10-methylacridine. The AD dyes are bond to AuNS *via* nitrogen atoms and LOD of the SERS nanotags (AuNS–CnAD–BSA) is as low as 0.4 pM. The intensity of these nanotags is approximately 5-fold higher than that of a commercial Raman reporter DTTC. The SERS images revealed the promising application of C5AD in biomedical measurement with a 785 nm laser as the excitation source. These significant results demonstrate the great potential of AD dyes as Raman reporters for biomedical imaging and selective detection and accurate resection of cancer cell. The AD dyes can be functionalized with pH responsive substituent and applied in the tracking pH variations and tumor delineation in the future experiments.

Conflicts of interest

There are no conflicts to declare.

Acknowledgements

This work was supported by the National Natural Science Foundation of China (51973017, 51773017), the State Key Laboratory for Advanced Metals and Materials (2018Z-06), and the Fundamental Research Funds for the Central Universities (FRF-DF-19-001).

Notes and references

1 Y. Wang and S. Schlucker, *Analyst*, 2013, **138**, 2224–2238.
2 X. Qian, X. H. Peng, D. O. Ansari, Q. Yin-Goen, G. Z. Chen, D. M. Shin, L. Yang, A. N. Young, M. D. Wang and S. Nie, *Nat. Biotechnol.*, 2008, **26**, 83–90.
3 V. Amendola and M. Meneghetti, *Adv. Funct. Mater.*, 2012, **22**, 353–360.
4 S. Harmsen, M. A. Bedics, M. A. Wall, R. Huang, M. R. Detty and M. F. Kircher, *Nat. Commun.*, 2015, **6**, 6570.
5 C. Andreou, V. Neuschmelting, D. F. Tschaharganeh, C. H. Huang, A. Oseledchyk, P. Iacono, H. Karabeber, R. R. Colen, L. Mannelli, S. W. Lowe and M. F. Kircher, *ACS Nano*, 2016, **10**, 5015–5026.
6 X. Jin, B. N. Khlebtsov, V. A. Khanadeev, N. G. Khlebtsov and J. Ye, *ACS Appl. Mater. Interfaces*, 2017, **9**, 30387–30397.
7 C. Song, F. Li, X. Guo, W. Chen, C. Dong, J. Zhang, J. Zhang and L. Wang, *J. Mater. Chem. B*, 2019, **7**, 2001–2008.
8 D. Jimenez de Aberasturi, A. B. Serrano-Montes, J. Langer, M. Henriksen-Lacey, W. J. Parak and L. M. Liz-Marzán, *Chem. Mater.*, 2016, **28**, 6779–6790.
9 D. Advanced MaterialsJimenez de Aberasturi, M. Henriksen-Lacey, L. Litti, J. Langer and L. M. Liz-Marzán, *Adv. Funct. Mater.*, 2020, **30**, 1909655.
10 Y. Wen, V. X. Truong and M. Li, *Nano Lett.*, 2021, **21**, 3066–3074.
11 S. Hua, S. Zhong, A. Hamed, J. He, D. Zhong, D. Zhang, X. Chen, J. Qian, X. Hu and M. Zhou, *Adv. Funct. Mater.*, 2021, 2100468, DOI: 10.1002/adfm.202100468.
12 M. A. Bedics, H. Kearns, J. M. Cox, S. Mabbott, F. Ali, N. C. Shand, K. Faulds, J. B. Benedict, D. Graham and M. R. Detty, *Chem. Sci.*, 2015, **6**, 2302–2306.
13 H. Kearns, M. A. Bedics, N. C. Shand, K. Faulds, M. R. Detty and D. Graham, *Analyst*, 2016, **141**, 5062–5065.
14 R. Javaid, N. Sayyadi, K. Mylvaganam, K. Venkatesan, Y. Wang and A. Rodger, *J. Raman Spectrosc.*, 2020, **51**, 2408–2415.
15 A. Samanta, K. K. Maiti, K. S. Soh, X. Liao, M. Vendrell, U. S. Dinish, S. W. Yun, R. Bhuvaneswari, H. Kim, S. Rautela, J. Chung, M. Olivo and Y. T. Chang, *Angew. Chem., Int. Ed.*, 2011, **50**, 6089–6092.
16 K. K. Maiti, U. S. Dinish, A. Samanta, M. Vendrell, K.-S. Soh, S.-J. Park, M. Olivo and Y.-T. Chang, *Nano Today*, 2012, **7**, 85–93.
17 T. Mahmood, A. Paul and S. Ladame, *J. Org. Chem.*, 2010, **75**, 204–207.
18 P. Yan, A. Xie, M. Wei and L. M. Loew, *J. Org. Chem.*, 2008, **73**, 6587–6594.
19 Y. Zhou, D. Chenchen, D. Jinshuai, Q. Ximei, C. Hui, W. Dong and H. Wanli, *China Patent*, CN107090190A, 2015.
20 Y. Zhou, D. Jinshuai, D. Yiqiang and Q. Ximei *China Patent*, CN104387790A, 2017.
21 H. Yuan, C. G. Khoury, H. Hwang, C. M. Wilson, G. A. Grant and T. Vo-Dinh, *Nanotechnology*, 2012, **23**, 075102.
22 L. Scarabelli, A. Sanchez-Iglesias, J. Perez-Juste and L. M. Liz-Marzan, *J. Phys. Chem. Lett.*, 2015, **6**, 4270–4279.
23 B. A. Armitage, in *DNA Binders and Related Subjects*, 2005, ch. 3, pp. 55–76, DOI: 10.1007/b100442.
24 J. P. G. IKvi, J. P. Marsault and J. Aubard, *J. Raman Spectrosc.*, 1993, 745–752.
25 B. Hao, X. Bu, J. Wu, Y. Ding, L. Zhang, B. Zhao and Y. Tian, *Microchem. J.*, 2020, **155**, 104736.
26 J. I. Millán, J. V. Garcia-Ramos, S. Sanchez-Cortes and R. Rodríguez-Amaro, *J. Raman Spectrosc.*, 2003, **34**, 227–233.